Further, Small-molecule Pyrolysis Products Derived from Chitin

Maryam Nikahd,[A] *Jiri Mikusek,*[A] *Martin G. Banwell,* [A,B,D] *Li-Juan Yu,*[C] *Michelle L. Coote*[C] *and Michael G. Gardiner* [A]

[A]Research School of Chemistry, Institute of Advanced Studies
The Australian National University, Canberra, ACT 2601, Australia
[B]Institute for Advanced and Applied Chemical Synthesis,
Jinan University, Guangzhou 510632, China
[C]ARC Centre of Excellence for Electromaterials Science, Research School of Chemistry,
The Australian National University, Canberra, ACT 2601, Australia
[D]Corresponding author. Email: Martin.Banwell@anu.edu.au

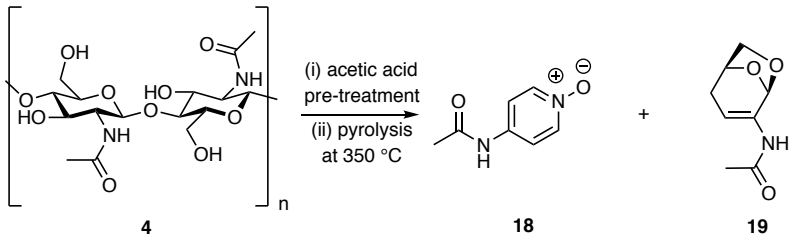

Abstract: In an ongoing study of the products formed on pyrolysis of chitin (**4**) under a range of conditions we now detail the isolation and characterization of the crystalline and hitherto undetected pyridine *N*-oxide **18** and enamide **19**. Pathways for the formation of these products have been proposed and subjected to both experimental and computational assessment.

† Dedicated to the memory of Professor Roy Jackson (Monash University), an outstanding

organic chemist and raconteur who brought imagination, rigor and fun to our discipline.

Introduction

As environmental considerations impinge ever more acutely on the development and commercialization of manifold chemical processes, there is an attendant and increasing interest in the identification of biomass-derived platform molecules (BDPMs)[1] that could serve as feedstocks for industry. A particularly notable and relatively recent development in this area has been the refinement of the process for the pyrolysis of acid-treated cellulose (**1**) (Figure 1), the most abundant biopolymer, and so allowing for the production of the BDPM levoglucosenone (**2**) at commercial scale.[2] Furthermore, the readily produced dihydro-derivative, *viz*. dihydrolevoglucosenone (**3**) and also known as Cyrene®, is now marketed as an industrial solvent and one that can serve as a less toxic alternative to *N*-methylpyrrolidinone (NMP).[2,3]

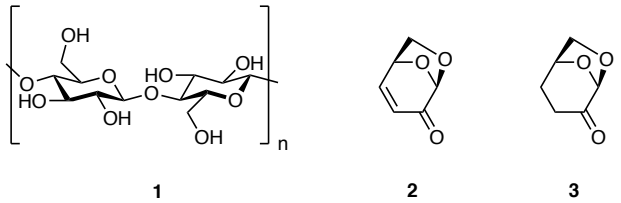

1 **2** **3**

Fig. 1. The structures of cellulose (**1**), its pyrolysis product levoglucosenone (**2**) and dihydrolevoglucosenone/Cyrene® (**3**)

Given the preponderance of nitrogen in many if not the majority of important small organic compounds and the absence of this element in cellulose, our group, together with various others,[4] have sought to explore ways by which chitin (**4**) (Figure 2) could be exploited so as to produce *N*-containing BDPMs. Chitin is the second most abundant biopolymer and comprised of linearly-linked repeating units of *N*-acetylglucosamine (NAG, **5**).[5] It is a major source of biologically fixed nitrogen and encountered in the exoskeleta of crustaceans, the cuticles of insects, plankton as well as the cell walls of fungi. Approximately 100 billon tons of chitin are believed to be produced by such organisms each year.[5] In our recently reported study[6] on the pyrolysis of certain treated forms of chitin we described the isolation of the hetero- and carbo-cyclic products **6**-**17**, all of which were rigorously characterized including, in most cases, by single-crystal X-ray analysis. In this same body of work we also presented possible mechanistic pathways by which these pyrolysis products could be formed and described various computational

studies that supported these proposals. In addition we noted that certain of these pyrolysis products could be characterized as dehydro-α-amino acid derivatives, a type of compound that has proven to be useful in various settings.[7,8]

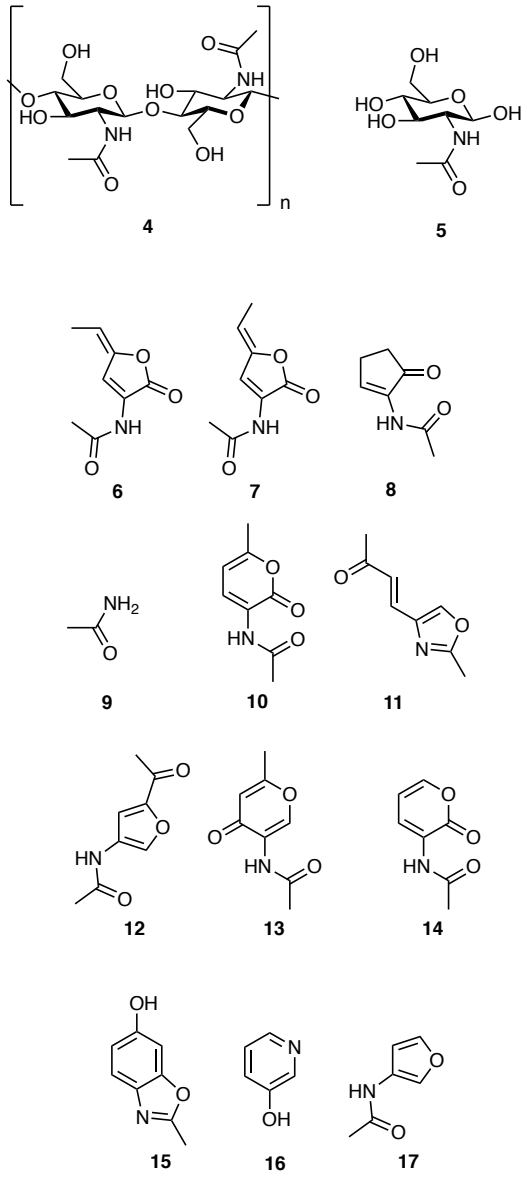

Fig. 2. The structures of chitin (**4**), the corresponding monomer NAG (**5**) and the previously reported pyrolysis products **6**-**17**.

In order to better understand the pathways by which chitin can undergo pyrolytic deploymerization, we continue to identify the products that can arise from such processes. The most recent outcomes of our endeavors in this regard are detailed here.

Results and Discussion

Pyrolytic and Synthetic Studies

Informed by the results of our earlier studies,[6] chitin was prepared for pyrolysis by heating a commercially derived sample of this in refluxing glacial acid for 72 h, cooling the resulting mixture, filtering it and then drying the retained solid under a gentle stream of compressed air. The resulting free-flowing solid was then mixed with an equal amount of acid-washed, chromatography grade sand in order to facilitate heat transfer during the pyrolysis process that was conducted in the apparatus described earlier.[6] Pyrolysis was carried out at 350 °C for 2 h at a (reduced) pressure of 5 mm Hg. The volatile products were collected in a liquid nitrogen trap and combined with the methanol washings of the cooled residue remaining in the pyrolysis zone. Upon subjection of the resulting material to conventional column chromatography then high performance liquid chromatography the previously unobserved pyrolysis products **18** (<1%) and **19** (<1%) were isolated (Scheme 1). Each of these crystalline compounds was subjected to spectroscopic examination including single-crystal X-ray analysis, details of which are provided in the Experimental and SI. While compound **19** is new, congener **18** has been described previously although only as the product of conventional (but unequivocal) chemical syntheses.[9] Significantly, a comparison of the ^{1}H and ^{13}C NMR spectral data recorded for the bulk material from which the crystal of compound **18** was derived for X-ray analysis did not match those reported by Puszko[9c] for this pyridine *N*-oxide. So, while the former spectrum suggested the presence of a C_2-symmetrical (C-4-substituted) pyridine *N*-oxide substructure within the bulk material, the ^{13}C NMR spectrum displayed six resonances rather than the five expected (and observed[9c]) for compound **18**. The high-resolution electron-impact mass spectrum of the bulk material displayed a prominent ion at *m/z* 151, the formula for which was shown to be $C_7H_7N_2O_2$. This may correspond to the $(M–H)^+$ species arising from compound **18** ($C_7H_8N_2O_2$) present in the bulk material. To date, the use of softer ionization techniques for acquiring mass spectral data on the bulk material has proved unedifying. As such, we conclude that the chromatographic fraction that has provided compound **18** also incorporates another pyrolysis product, the structure of which remains unclear at the present time.

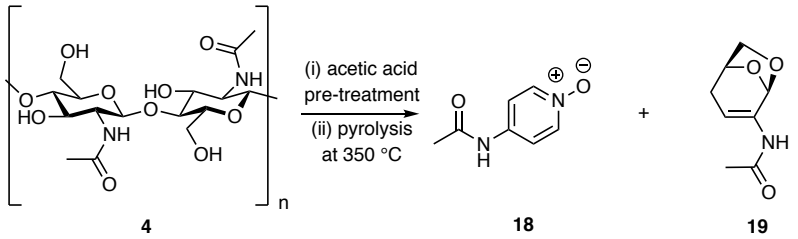

Scheme 1. Products **18** and **19** obtained from the pyrolysis of chitin (**4**) that had been treated with glacial acetic acid.

Each of these small molecule pyrolysis products has its own intriguing features. First of all, the former (**18**) is the only one we have isolated thus far that contains two nitrogen atoms. Compound **19**, on the other hand, is the first we have encountered that retains any of the stereogenic centers associated with the starting material **4**. A key question that immediately emerges as a result of these observations is how are these products formed. One possible pathway leading from the previously observed[6] pyrolysis products **9** and **16** to compound **18** is shown in Scheme 2. Thus, the acid-catalyzed dehydration of 3-hydroxypyridine (**16**) might be expected to give 3,4-pyridyne (**20**) that is itself intercepted in a regioselective manner by acetamide (**9**), the most abundant, by far, of the pyrolysis products we have observed to date. This "interception", involving the overall addition of aryne **20** to the N-H σ-bond of the amide would then afford the observed *N*-aryl acetamide **18**.

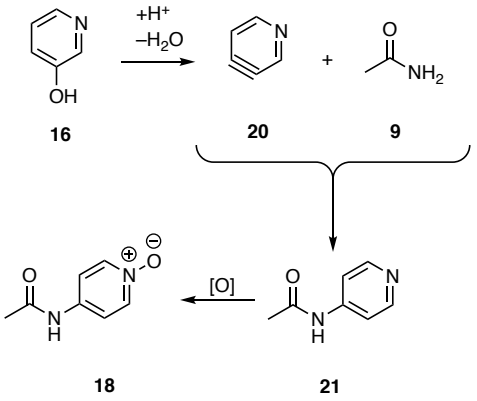

Scheme 2. A possible pathway for the formation of compound **18** from 3-hydroxypyridine (**16**) and acetamide (**9**).

An obvious variation on this possibility is one (Scheme 3) wherein the oxidation of pyridine **16** takes places first with the product *N*-oxide **22** then undergoing dehydration.

The 3,4-pyridyne *N*-oxide (**23**) thus formed could now react with acetamide in a manner analogous to that suggested above and so forming, once again, the observed product **18**.

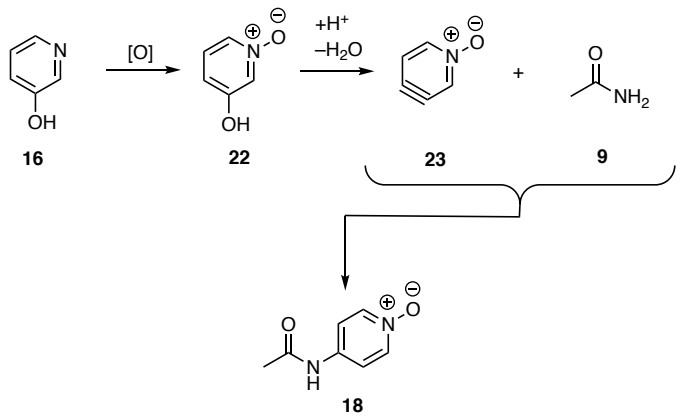

Scheme 3. An alternative pathway for the formation of compound **18** from 3-hydroxypyridine (**16**) and acetamide (**9**).

Pyridynes are reactive intermediates that have garnered attention over many decades, but particularly in recent times,[10] as rather readily generated species that can be exploited in various contexts. Such studies have revealed that the parent 3,4-pyridyne is more stable than its 2,3-isomer. Furthermore, each of these has been shown to react in a regioselective manner with a range of nucleophiles including amines. In the former case, the 4-amino-substituted pyridine is formed preferentially. Pyridyne *N*-oxides do not appear to have been studied experimentally but a theoretical study[11] suggests that they too should react with added electrophiles in a manner similar to that observed with the corresponding "parent" systems.

In an effort to provide experimental support for the first of the above proposals an equimolar mixture of commercially available samples of 3-hydroxypyridine (**16**) and acetamide (**9**) was subjected to pyrolysis in the presence of acid-treated sand at 350 °C. However, compound **18** could not be detected in the product mixture. Indeed, the only materials recovered from this process were the starting materials **9** and **16**. Since the *N*-oxide **22** is not a known compound it has not been possible, at this point, to examine the outcomes of its co-pyrolysis with acetamide (**9**). Nevertheless, the computational studies detailed in the following section suggest that this could be a worthwhile experimental pursuit.

A possible pathway for the formation of product **19** from chitin is shown in Scheme 4. This starts with the fragmentation of the biopolymer in the manner we have suggested[6] previously to give the oxonium ion **24**. Cyclisation of the latter species would then deliver 2-acetamido-1,6-anhydro-2-deoxy-β-D-glucopyranose (**25**), a compound that has been detected in chitin associated with fossil arthropods and upon subjecting the biopolymer to Curie-point pyrolysis/gas chromatographic analysis.[12] In keeping with our earlier proposal[6] regarding the formation of pyrolysis products **11** and **15** from chitin, we suggest that *trans*-diol **25** reacts with an α-dicarbonyl compound such as glyoxal to produce the cyclic *bis*-hemiacetal **26** that itself undergoes the illustrated cycloreversion process and thereby affording alkene **27** together with two molecules of formic acid. Finally, double-bond migration within compound **27** would afford the observed isomer **19**.

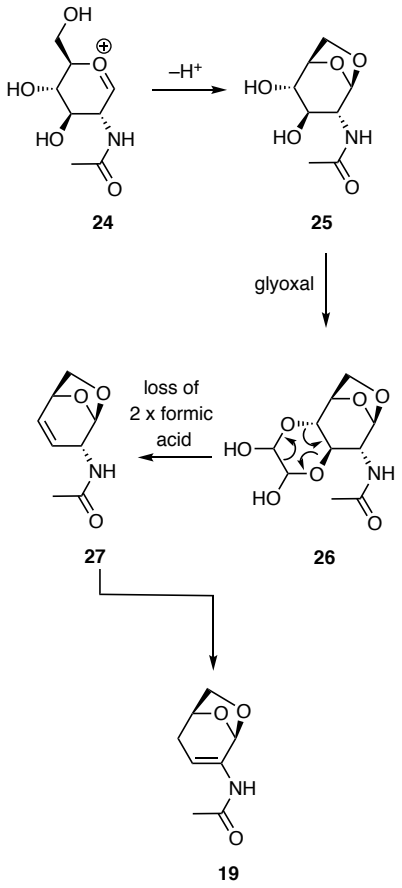

Scheme 4. A possible pathway for the formation of compound **19** from chitin.

The pivotal features of the proposal shown in Scheme 4 are the formation and fragmentation of intermediate **26**. In this context it is worth noting that α-dicarbonyl compounds are known to form during the thermal decomposition of monosaccharides.[13]

Furthermore, we have observed[14] that under flash vacuum pyrolytic (FVP) conditions, Ley-type di-acetals[15] derived from cyclic *trans*-diols undergo cycloreversion reactions of the type shown to give the corresponding cycloalkene. Accordingly, we sought to study this process using a model compound. To that end, NAG (**5**) (Scheme 5) was converted, following a procedure defined by Wan *et al*,[16] into the known derivative **28** (84%) by treating the former compound with methanol in the presence acidified Amberlyst resin. Product **28** was immediately treated with a mixture of butan-2,3-dione, trimethyl orthoformate and camphorsulfonic acid (CSA) and thereby delivering the target model compound **29**, a 1,2-diacetal, in 66% yield. The NMR spectral data recorded on this product matched those reported previously[16] and final confirmation of its structure was also secured by single-crystal X-ray analysis, details of which are presented in the Experimental Section and the SI.

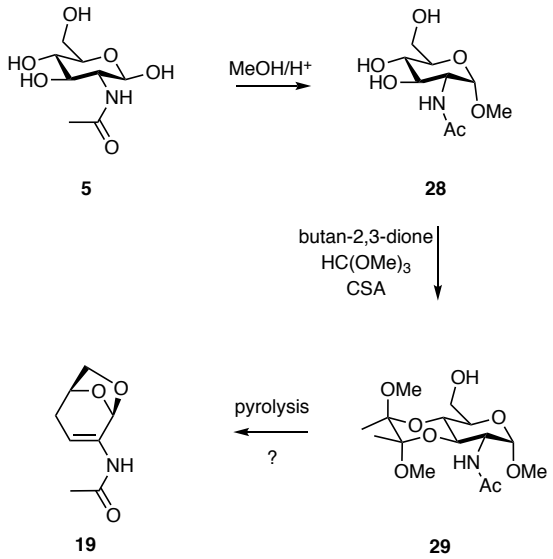

Scheme 5. The synthesis of compound **29** as a substrate for testing the proposed pyrolytic origins of compound **19**.

Upon subjecting an acid-treated sample of compound **29** (admixed with chromatography-grade sand) to pyrolysis at 350 °C under standard conditions[6] no clear transformations were observed. Certainly, no evidence for the formation of compound **19** was obtained. In fact, the starting 1,2-diacetal was the only characterizable material obtained after work-up. The rather robust nature of compound **29** revealed by this outcome prompted a further aspect of the computational studies described below. Specifically, by such means we sought to gain insights into how the nature of the substituents associated with the 1,2-diacetal residue and the manner in which it is annulated to other ring systems might

influence the ease, or otherwise, with which the proposed cycloreversion reaction takes place.

Computational Studies

The initial focus of our computational studies was on the possible modes of formation of the pyridine *N*-oxide **18** shown in Scheme 2 and its counterpart **22** shown in Scheme 3. To that end, the nature of the oxidant involved in the formation of each of these had to be considered. In principle, this could be hydrogen peroxide, peracetic acid (arising from the reaction of hydrogen peroxide with either acetamide, a co-pyrolysis product, or any acetic acid occluded in the chitin after the pre-treatment process) or ozone. Certainly, these oxidants are known to effect such conversions.[17-20] While molecular oxygen does not do so, at least under conventional conditions, it was included in initial calculations but quickly discounted as a possibility because of the distinctly unfavourable energetics. Using high-level *ab initio* molecular orbital theory-based calculations (see SI for details) the reaction profiles for the pathways shown in Schemes 2 and 3 were generated and these are shown in Schemes 6 and 7, respectively.

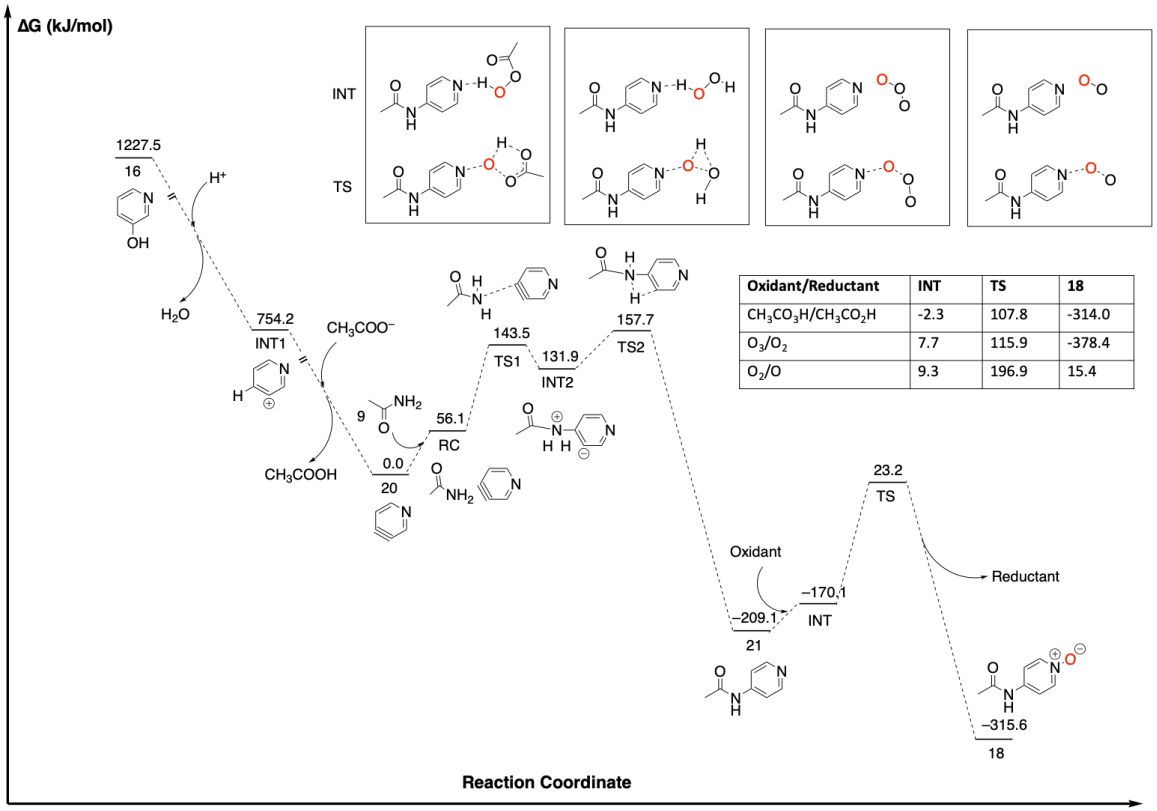

Oxidant/Reductant	INT	TS	18
CH_3CO_3H/CH_3CO_2H	-2.3	107.8	-314.0
O_3/O_2	7.7	115.9	-378.4
O_2/O	9.3	196.9	15.4

Scheme 6. The calculated energy profile for the formation of pyrolysis product **18** by the pathway shown in Scheme 2. The oxidant shown here is H_2O_2, corresponding results for other oxidants are shown in the inserted table.

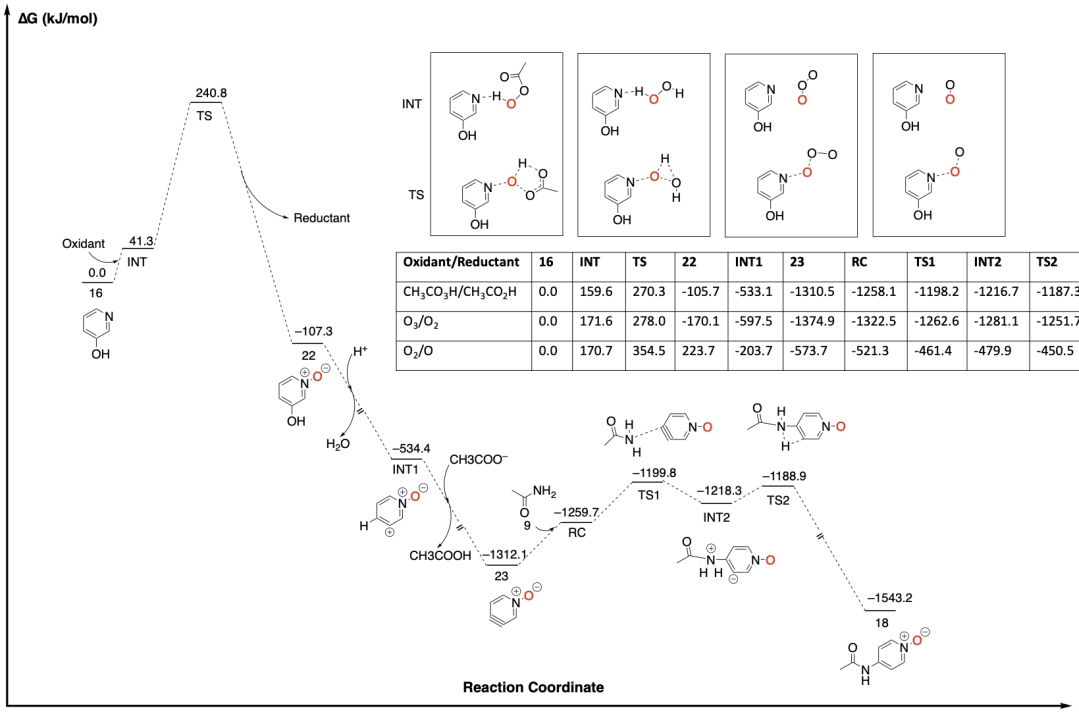

Oxidant/Reductant	16	INT	TS	22	INT1	23	RC	TS1	INT2	TS2	18
CH_3CO_3H/CH_3CO_2H	0.0	159.6	270.3	-105.7	-533.1	-1310.5	-1258.1	-1198.2	-1216.7	-1187.3	-1541.6
O_3/O_2	0.0	171.6	278.0	-170.1	-597.5	-1374.9	-1322.5	-1262.6	-1281.1	-1251.7	-1606.0
O_2/O	0.0	170.7	354.5	223.7	-203.7	-573.7	-521.3	-461.4	-479.9	-450.5	-96.2

Scheme 7. The calculated energy profile for the formation of pyrolysis product **18** by the pathway shown in Scheme 3. The oxidant shown here is H_2O_2, corresponding results for other oxidants are shown in the inserted table.

It is clear from these profiles that pyridyne formation through stepwise dehydration of 3-hydroxypyridine (**16**) (Scheme 2) is favoured to a significant extent over the equivalent process starting from the corresponding *N*-oxide **22** (Scheme 3). Furthermore, regardless of the timing of the necessary oxidation at nitrogen, hydrogen peroxide would appear to be the most favoured species for effecting this transformation, at least in energetic terms. The related issue that was examined from a computational perspective concerned the regioselectivity of the reaction of the intermediate pyridynes **20** and **23** with acetamide and whether formation of the 4-acetamido-substituted system was preferred over its 3-substituted isomer. Intriguingly, as revealed in Scheme 8 if pyridyne **20** (Scheme 2) is the intermediate involved in the pathway involved in formation of final product **18** then there should be some preference for formation of its 3-substituted isomer, *viz*. 3-acetamidopyridine 1-oxide, a species we have not detected in any chitin pyrolysis product mixture generated thus far. In contrast, as shown in Scheme 9, if pyridyne *N*-oxide **23** (Scheme 3) is the intermediate intercepted by acetamide (an energetically less likely possibility – see Scheme 7) then formation of compound **18** would be preferred.

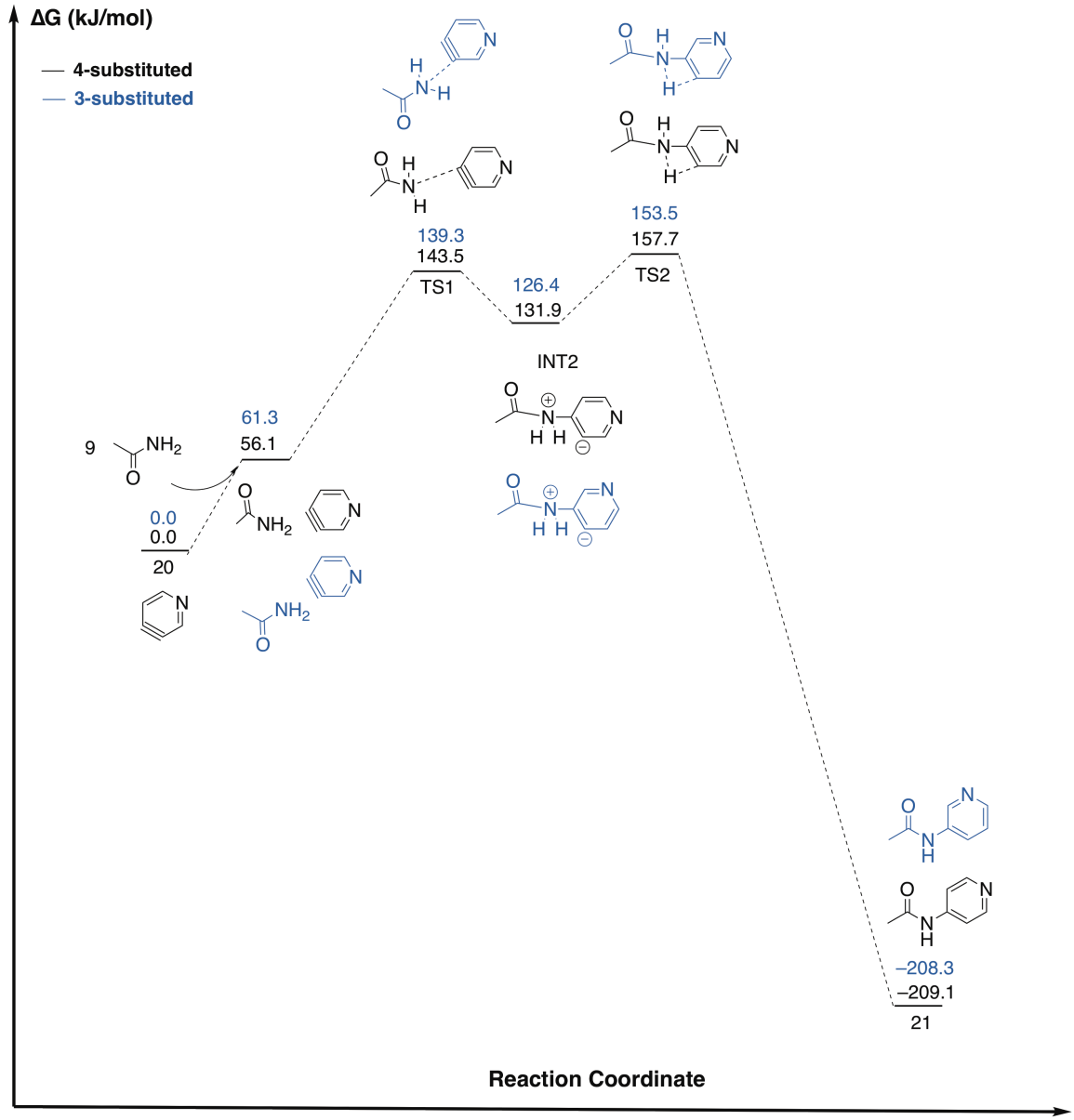

Scheme 8: The calculated energy profiles for the formation of 3- (top numbers) and 4- (bottom numbers) acetamidopyridine through reaction of 3-pyridyne (**20**) with acetamide.

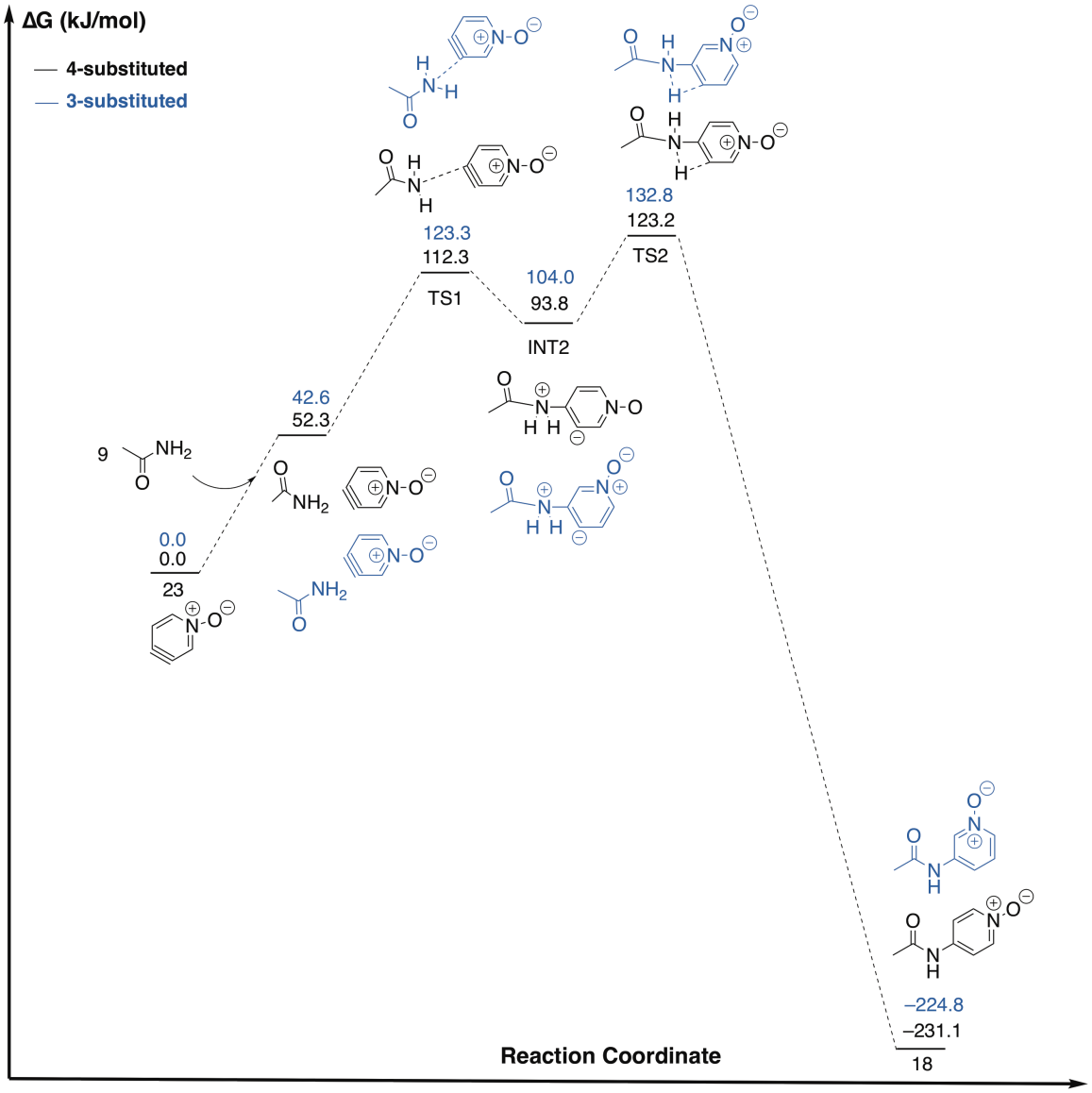

Scheme 9: The calculated energy profiles for the formation of compound **18** (bottom numbers) and its regioisomer 3-acetamidopyridine 1-oxide (top numbers) through reaction of 3-pyridyne 1-oxide (**23**) with acetamide.

Another facet of the computational studies reported here concerned the structural factors that could influence the energetics of the proposed fragmentation process leading from, for example, the *trans*-diol derivative **26** to alkene **27** (Scheme 4). In refined form, such a process could provide a useful means for effecting the deoxygenation of biomass, a topic of particular interest in connection with the development of non-petroleum derived chemical feedstocks.[21] Specifically, then, the four conversions shown in Scheme 10 were evaluated computationally, the results of which were thought likely to provide insights into the impacts of both the substituents associated with the 1,2-diacetal moiety and the

framework (mono-or bi-cyclic in these cases) to which this is annulated. Given the large size of these systems, for these species shown in Scheme 10 M06-2X/6-31+G(d,p) energies were presented in place of G3(MP2,CC) used elsewhere.

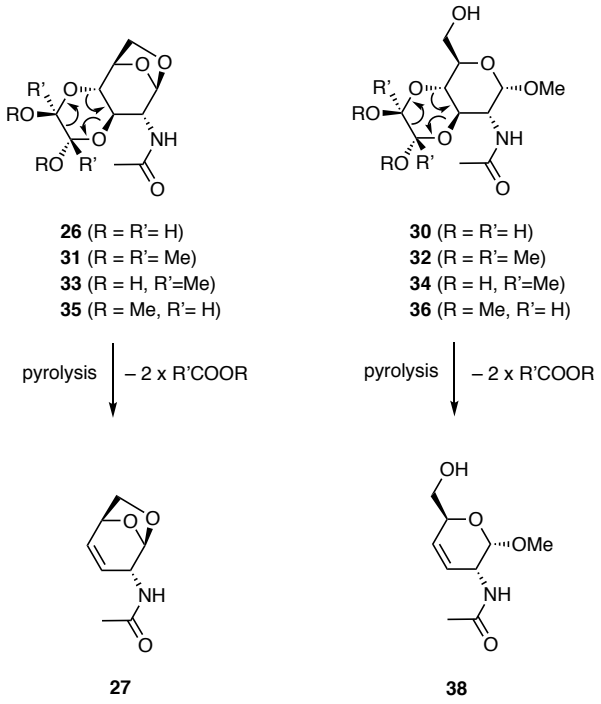

Scheme 10: Eight possible substrates (**26**, **30**-**36**) and their respective potential pyrolysis products (**27** and **38**) arising via the illustrated fragmentation reactions.

As revealed in Table 1, both of the structural features just mentioned affect the activation energies as well as the exothermicities of the illustrated and pyrolytically-induced fragmentation processes. So for example, replacing hydroxyl groups with methoxy groups can increase the activation barrier by almost 40 kJ/mol (compare Entries 1 and 3 as well Entries 2 and 4). In contrast, the mode of annulation of the 1,2-diacetal moiety has much more modest impacts, the most significant being one in which the mono-annulated system **38** is disfavoured, in terms of activation energy, by 12 kJ/mol over that leading to 1,6-anhydro-bridged system **27** (compare entries 3 and 4). Interestingly, those processes leading to formic or acetic acid by-products are significantly less exothermic than the ones that afford the corresponding methyl esters.

Table 1: Calculated activation energies and exothermicities associated with the conversions shown in Scheme 10.

Entry	Substrate	Product	$\Delta G^{\ddagger}$	ΔG
1	**26**	**27**	**327.6**	**–220.7**
2	**30**	**38**	**319.8**	**–253.2**
3	**31**	**27**	**355.6**	**–299.7**
4	**32**	**38**	**367.6**	**–312.1**
5	**33**	**27**	**349.5**	**–9.6**
6	**34**	**38**	**351.6**	**–31.5**
7	**35**	**27**	**345.4**	**–237.6**
8	**36**	**38**	**345.8**	**–252.8**

$\Delta G^{\ddagger}$ and ΔG values are given in kJ/mol

These computational results will inform our ongoing studies in which we seek to develop the thermolytic fragmentation reactions of di-acetals as a means for the deoxygenation of *trans*-diols such as compounds **25** and **28** as well as biomass more generally.

Conclusion

The present work further highlights the diversity of reaction pathways that can take place on pyrolysis of the nitrogen-containing biopolymer chitin. It also suggests that some control over these can be achieved by the manner in which the biopolymer is treated prior to pyrolysis. The mechanistic proposals advanced here will be the subject of further experimental studies and it is hoped the outcomes of these will help inform how a channeling of these pathways might be achieved. Realizing such objectives should assist in deriving greater value from the biopolymer chitin that, at the present time, remains a distinctly underutilized resource.

Experimental

General Experimental Protocols

Unless otherwise specified, proton (^{1}H) and proton-decoupled carbon [^{13}C{^{1}H}] NMR spectra were recorded at room temperature in base-filtered $CDCl_3$ on a Varian spectrometer operating at 400 MHz for proton and 100 MHz for carbon nuclei. For ^{1}H NMR spectra, signals arising from the residual protio-forms of the solvent were used as the internal standards. ^{1}H NMR data are recorded as follows: chemical shift (δ) [multiplicity, coupling constant(s) *J* (Hz), relative integral] where multiplicity is defined as: s = singlet; d = doublet; t = triplet; q = quartet; m = multiplet or combinations of the above. The signal due to residual $CHCl_3$ appearing at δ_H 7.26 and the central resonance of the $CDCl_3$ "triplet" appearing at δ_C 77.16 were used to reference ^{1}H and ^{13}C{^{1}H} NMR spectra, respectively. Infrared spectra (ν_{max}) were recorded on a Perkin–Elmer 1800 Series FTIR Spectrometer. Samples were analysed as thin films. Low-resolution ESI mass spectra were recorded on a single quadrupole liquid chromatograph-mass spectrometer, while high-resolution measurements were conducted on a time-of-flight instrument. Low- and high-resolution EI mass spectra were recorded on a magnetic-sector machine. Melting points were measured on a Reichert melting point microscope and are uncorrected. Analytical thin layer chromatography (TLC) was performed on aluminum-backed 0.2 mm thick silica gel 60 F_{254} plates as supplied by Merck. Eluted plates were visualized using a 254 nm UV lamp and/or by treatment with a suitable dip followed by heating. These dips included phosphomolybdic acid : ceric sulfate : sulfuric acid (conc.) : water (37.5 g : 7.5 g : 37.5 g : 720 mL) or potassium permanganate : potassium carbonate : 5% sodium hydroxide aqueous solution : water (3 g : 20 g: 5 mL : 300 mL). Flash chromatographic separations were carried out following protocols defined by Still *et al*.[22] with silica gel 60 (40–63 □m) as the stationary phase and using the AR- or HPLC-grade solvents indicated. Reverse-phase HPLC purifications were carried out using an Alltima C18 250 × 22 mm column using, as the eluting solvent, 3:7 v/v water/acetonitrile at a flow rate of 10 ml/min. and ambient temp. Starting materials and reagents were generally available from the Sigma–Aldrich, Merck, TCI, Strem or Lancaster Chemical Companies and were used as supplied. Drying agents and other inorganic salts were purchased from the AJAX, BDH or Unilab Chemical Companies. Tetrahydrofuran (THF), methanol and dichloromethane were dried using a Glass Contour solvent purification system that is based upon a technology originally described by Grubbs *et al*.[23] Petroleum ether refers to

the fraction boiling between 40 and 60 °C. Where necessary, reactions were performed under a nitrogen atmosphere.

Specific Chemical Transformations

*4-Acetamidopyridine 1-oxide (**18**) and* N-*((1*S*,5*R*)-6,8-Dioxabicyclo[3.2.1]oct-3-en-4-yl)acetamide (**19**).*

A 250 mL round bottomed flask was charged with chitin (10.0 g) then glacial acetic acid (150 mL). The resulting slurry was heated, with vigorous stirring, under reflux (*ca*. 118 °C) for 72 h then cooled to room temperature before being filtered. The wet solid thus obtained was dried under a stream of compressed air for 2 days then the free-flowing material intimately mixed with acid-washed, chromatography grade sand (20 g). The resulting material was subjected to pyrolysis at 350 °C for 2 h under reduced pressure (5 mm of Hg) using the apparatus described elsewhere.[6] The distillate obtained together with the methanol washings of the residues remaining in the pyrolysis zone yielded, after concentration on rotary evaporator, a brown oil (4.88 g). This was subjected to flash chromatography (silica gel, 2:8→9:1 v/v ethyl acetate/petroleum ether then 0.5:9.5 v/v methanol/ethyl acetate gradient elution). Concentration of the appropriate fraction (R_f = 0.15 in 0.5:9.5 v/v methanol/chloroform) and subjection of the resulting light-yellow oil (73 mg) to reverse-phase HPLC (on a Grace Alltima C18 250 x 22 mm 5□m column - P/N 81105 - using 3:7 v/v water/acetonitrile as the eluting solvent at a flow rate of 10 mL/min) yielded a mixture of compounds **18** and **19** (9.4 mg, R_t = 9.653 min). This material was subjected to flash column chromatography (silica gel, 0.2:9.8 → 0.5:9.5 v/v methanol/chloroform gradient elution) to yield two fractions, A and B.

Concentration of fraction A (R_f = 0.3 in 1:9 v/v methanol/chloroform) yielded a white solid than upon recrystallisation (methanol) gave the bulk material (1.3 mg) from which the crystal of compound **18** was selected for single-crystal X-ray analysis. This bulk material was a white, crystalline solid, m.p. = 132-140 °C. ^{1}H NMR (400 MHz, CD_3OD) δ 7.30 (d, J = 7.5 Hz, 2H), 6.72 (d, J = 7.5 Hz, 2H), 2.08 (s, 3H); ^{1}H NMR [400 MHz, $(CD_3)_2SO$] δ 9.60 (broad s, 1H), 9.10 (broad s, 1H), 7.32 (d, J = 7.5 Hz, 2H), 6.65 (d, J = 7.5 Hz, 2H), 1.96 (s, 3H); $^{13}C\{^1H\}$ NMR (100 MHz, CD_3OD) δ 171.3, 155.4, 131.7, 123.3, 116.2, 23.5; $^{13}C\{^1H\}$ NMR [400 MHz, $(CD_3)_2SO$] δ 167.4, 153.1, 131.0, 120.8, 115.0, 23.7; IR υ_{max} 2923, 1575, 1478, 1446, 1276 ,1238, 1103, 1045, 800, 704, 637 cm^{-1}; HRMS (EI, 70 eV) calcd for $C_7H_7N_2O_2$ $(M - H\bullet)^+$ 151.0508, found 151.0510.

Concentration of fraction B (R_f = 0.2 in 0.2:9.8 v/v methanol/chloroform) yielded a white solid than upon recrystallisation (methanol) afforded compound **19** (1.2 mg) as a white, crystalline solid, m.p. = 95-102 °C, $[\alpha]_D$ = +132.0 (*c* = 0.1, $CHCl_3$). ^{1}H NMR (400 MHz, $CDCl_3$) δ 6.51 (broad s, 1H), 5.90 (s, 1H), 5.52 (s, 1H), 4.69 (t, *J* = 5.2 Hz, 1H), 3.99–3.93 (complex m, 1H), 3.74–3.69 (complex m, 1H), 2.87–2.78 (complex m, 1H), 2.06 (s, 3H), 1.96 (dd, *J* = 17.7 and 5.0 Hz, 1H); ^{13}C{^{1}H} NMR (100 MHz, CD_3OD) δ 168.7, 134.4, 106.6, 97.4, 72.0, 68.6, 31.1, 24.3; IR υ_{max} 3279, 2925, 1663, 1375, 1108 cm^{-1}; MS (ESI, +ve) *m*/*z* 129 (M + Na$^+$, 100%); HRMS (ESI, +ve) calcd for $C_8H_{11}NO_3Na$ (M + Na$^+$) 192.0637, found 192.0630.

N-*((2*S*,3*S*,4a*S*,5*R*,7*S*,8*R*,8a*R*)-5-(Hydroxymethyl)-2,3,7-trimethoxy-2,3-dimethylhexa-hydro-5*H*-pyrano[3,4-*b*][1,4]dioxin-8-yl)acetamide (**29**).*

Step i: A 250 mL round-bottomed flask equipped with magnetic stirring bar was charged with *N*-acetylglucosamine (**5**) (5.0 g, 22.6 mmol), Amberlyst-H$^+$ (8.0 g) and methanol (120 mL). The resulting and magnetically stirred suspension was heated under a reflux for 21 h and during the first 1.5 h of this period a clear reaction mixture formed. The cooled reaction mixture was was filtered (to remove the acidic resin) and the concentrated under reduced pressure and thereby affording compound **28**[16] (4.44 g, 84% yield) as a white, crystalline solid. This material was immediately subjected to *step ii* of the reaction sequence as detailed below.

Step ii: A 250 mL round-bottomed flask equipped with magnetic stirring bar and charged with acetal **28** (4.44 g, 18.9 mmol), butane-2,3-dione (2 mL, 22.7 mmol), trimethyl orthoformate (7.9 mL, 71.8 mmol), camphorsulfonic acid (302 mg, 1.3 mmol) and methanol (80 mL). The ensuing mixture was heated under reflux for 72 h then cooled, treated with triethylamine (420 □L, 3 mmol), stirred for 10 min at ambient temperatures then concentrated under reduced pressure under reduced pressure. The residue thus obtained was subjected to flash column chromatography (silica gel, ethyl acetate elution) to yield, after concentration of the appropriate fractions (R_f = 0.1), an orange solid than upon recrystallisation (methanol) gave compound **29**[16] (4.16 g, 66%) as an orange-yellow, crystalline solid, m.p. = 80-89 °C, $[\alpha]_D$ = +178.8 (*c* = 1.0, $CHCl_3$). ^{1}H NMR (400 MHz, CD_3OD) δ 4.64 (d, *J* = 3.6 Hz, 1H), 4.13 (dd, *J* = 11.1 and 3.6 Hz, 1H), 3.91 (dd, *J* = 11.2 and 8.8 Hz, 1H), 3.81–3.75 (complex m, 1H), 3.68–3.61 (complex m, 3H), 3.40 (s, 3H), 3.25 (s, 3H), 3.24 (s, 3H), 1.97 (s, 3H), 1.25 (s, 3H), 1.24 (s, 3H); ^{13}C{^{1}H} NMR (100 MHz, CD_3OD) δ 173.5, 101.1, 101.0, 100.2, 71.8, 68.7, 68.4, 61.5,

55.6, 52.4, 48.3, 22.4, 18.1, 18.0. These data are in complete accord with those reported in the literature.[16]

Crystallographic Studies

Crystallographic Data

Compound **18**. $C_7H_{13}N_2O_2$, M = 157.19, T = 100 K, orthorhombic, space group *Pbcm*, Z = 4, a = 8.5710(4) Å, b = 11.7570(6) Å, c = 7.2040(5) Å; V = 725.94(7) Å^3, D_x = 1.438 Mg m^{-3}, 857 unique data ($2\theta_{max}$ = 54.89°), R = 0.0630 [for 768 reflections with $I > 2.0\sigma(I)$]; Rw = 0.1923 (all data), S = 1.055.

Compound **19**. $C_8H_{11}NO_3$, M = 169.18, T = 150 K, orthorhombic, space group, $P2_12_12_1$, Z = 8, a = 9.5321(18) Å, b = 9.8389(7) Å, c = 17.5090(17) Å; V = 1642.1(2) Å^3, D_x = 1.369 Mg m^{-3}, 2837 unique data ($2\theta_{max}$ = 133.11°), R = 0.0457 [for 2118 reflections with $I > 2.0\sigma(I)$]; Rw = 0.0962 (all data), S = 0.975.

Compound **29**. $C_{15}H_{27}NO_8$, M = 349.37, T = 150 K, orthorhombic, space group, $P2_12_12_1$, Z = 4, a = 11.41220(10) Å, b = 11.48500(10) Å, c = 13.24190(10) Å; V = 1735.60(3) Å^3, D_x = 1.337 Mg m^{-3}, 3489 unique data ($2\theta_{max}$ = 147.56°), R = 0.0258 [for 3473 reflections with $I > 2.0\sigma(I)$]; Rw = 0.0668 (all data), S = 1.049.

Structure Determinations.

Data for compound **18** were collected at the Australian Synchrotron on the MX2 beamline (λ = 0.71075 Å).[24] Data for compounds **19** and **29** were collected on a SuperNova machine using CuKα, radiation, graphite monochromator (λ = 1.54184 Å) with data collection, cell refinement and data reduction employing the CrysAlis PRO program.[25] SHELXT[26] and SHELXL[27] were used for structure solution and refinement of all three structures. Atomic coordinates, bond lengths and angles, and displacement parameters have been deposited at the Cambridge Crystallographic Data Centre (CCDC nos. 2003422-2003424). These data can be obtained free-of-charge via www.ccdc.cam.ac.uk/data_request/cif, by emailing data_request@ccdc.cam.ac.uk, or by contacting The Cambridge Crystallographic Data Centre, 12 Union Road, Cambridge CB2 1EZ, UK; fax: +44 1223 336033.

Accession Codes

Theoretical Studies

Methodologies

Geometries were optimized at the M06-2X/6-31+G(d,p) level of theory[28] and frequencies were also calculated at this level. Geometries were verified either as local minima or transition states. Entropies, thermal corrections, and zero-point vibrational energies were scaled using the recommended scaling factors.[29] Single-point energies were calculated using the high-level composite ab initio method G3(MP2,CC) to improve accuracy.[30] This level of theory has been shown previously to provide accurate reaction energies and barrier heights.[6] All standard ab initio molecular orbital theory and density functional theory (DFT) calculations were carried out using the Gaussian 16[31] and Molpro 2019[32] software packages

Supplementary Material

This contains ORTEPs derived from X-ray analyses of compounds **18**, **19** and **29** together with copies of the NMR spectra of compounds **19** and **29** as well as the NMR spectra of the bulk material from which the crystal of compound **18** was extracted for X-ray analysis. Full details of the reported calculations together with raw computational data are also provided. This material is available on the Journal's website.

Conflicts of Interest

The authors declare no conflicts of interest.

Acknowledgments

We thank the Australian Government and Circa Pty Ltd for the provision of an Innovations Connections grant. Funding from the Australian Research Council is gratefully acknowledged (including through grants FL170100041 and CE140100012) as is support (to MN) from the Islamic Government of Iran. Parts of this research were undertaken using the MX2 beamline at the Australian Synchrotron (part of ANSTO) and made use of the Australian Cancer Research Foundation (ACRF) detector.

References

[1] (a) J. S. Luterbacher, D. M. Alonso, J. A. Dumesic, *Green Chem*. **2014**, *16*, 4816-4838; (b) N. Brun, P. Hesemann, D. Esposito, *Chem. Sci*. **2017**, *8*, 4724-4738; (c) J.-V. Bomtempo, F. C. Alves, F. de Almeida Oroski, *Faraday Discuss*. **2017**, *202*, 213-225; (d) Y. Lie, P. Ortiz, R. Vendamme, K. Vanbroekhoven, T.J. Farmer, *Ind. Eng. Chem. Res.* **2019**, *58*, 15945−15957.

[2] J. E. Camp, *ChemSusChem*. **2018**, *11*, 3048-3055.

[3] https://cen.acs.org/business/biobased-chemicals/New-solvent-Cyrene-takes-NMP/97/i22 (accessed 13/05/ 2020).

[4] For some representative reports, see: (a) X. Chen, Y. Gao, L. Wang, H. Chen, N. Yan, *ChemPlusChem* **2015**, *80*, 1565-1572; (b) X. Gao, X. Chen, J. Zhang, W. Guo, F. Jin, N. Yan, *ACS Sustainable Chem. Eng*. **2016**, *4*, 3912-3920; (c) C. Liu, H. Zhang, R. Xiao, S. Wu, *Carbohydrate Polymers*, **2017**, *156*, 118-124; (d) M. J. Hülsey, H. Yang, N. Yan, *ACS Sustainable Chem. Eng*. **2018**, *6*, 5694-5707; (e) P. Zhang, H. Hu, H. Tang, Y. Yang, H. Liu, Q. Lu, X. Li, N. Worasuwannarak, H. Yao, *Renewable Energy*, **2019**, *139*, 730-738.

[5] (a) N. Yan, X. Chen, *Nature*, **2015**, *524*, 155-158; (b) A. Jardine, S. Sayed, *Curr. Opin. Green Sustainable Chem*. **2016**, *2*, 34-39 and references cited therein.

[6] M. Nikahd, J. Mikusek, L.-J. Yu, M. L. Coote, M. G. Banwell, C. Ma, M. G. Gardiner, *J. Org. Chem*. **2020**, *85*, 4583-4593.

[7] J. W. Bogart, A. A. Bowers, *Org. Biomol. Chem*. **2019**, *17*, 3653-3669 and references cited therein.

[8] For examples of efforts to exploit certain chitin pyrolysis products as starting points in chemical synthesis programs, see: (a) Y. Liu, C. Stähler, J. N. Murphy, B. J. Furling, F. M. Kerton, *ACS Sustainable Chem. Eng*. **2017**, *5*, 4916-4922; (b) T. T. Pham, X. Chen, N. Yan, J. A. Sperry, *Monatsh Chem*. **2018**, *149*, 857-861; (c) A. D. Sadiq, X. Chen, N. Yan, J. Sperry, *ChemSusChem* **2018**, *11*, 532-535; (d) T. T. Pham, G. Gözaydin, T. Söhnel, N. Yan, J. Sperry, *Eur. J. Org. Chem*. **2019**, 1355-1360; (e) T. T. Pham, X. Chen, T. Söhnel, N. Yan, J. Sperry, *Green Chem*. **2020**, *22*, 1978-1984.

[9] (a) T. Kubota, H. Miyazaki, *Bull. Chem. Soc. Jpn*, **1966**, *39*, 2057-2062; (b) Y. Rabinsohn, A. J. Acher, D. Shapiro, *J. Org. Chem*. **1973**, *38*, 202-204; (c) A. Puszko, K. Laihia, E. Kolehmainen, Z. Talik, *Struct. Chem*. **2013**, *24*, 333-337.

[10] (a) A. E. Goetz, N. K. Garg, *J. Org. Chem*. **2014**, *79*, 846-851; (b) T. C. McMahon, J. M. Medina, Y.-F. Yang, B. J. Simmons, K. N. Houk, N. K. Garg, *J. Am. Chem. Soc*. **2015**, *137*, 4082-4085; (c) A. E. Goetz, T. K. Shah, N. K. Garg, *Chem. Commun*. **2015**, *51*, 34-45; (d) S. K. Thompson, T. R. Hoye, *J. Am. Chem. Soc*. **2019**, *141*, 19575-19580.

[11] N. Mariet, M. Ibrahim-Ouali, J.-L. Parrain, M. Santelli, *J. Mol. Struc. (Theochem)*, **2004**, *679*, 53-58.

[12] A. van der Kaaden, J. J. Boon, J. W. de Leeuw, F. de Lange, P. J. W. Schuyl, H.-R. Schulten, U. Bahr, *Anal. Chem*. **1984**, *56*, 2161-2165; (b) A. Bierstedt, B. A. Staniewicz, D. E. G. Briggs, R. P. Evershed, *Analyst*, **1998**, *123*, 139-145.

[13]. O. Novotny, K. Cejpek, J. Velisek, *Czech J. Food Sci*. **2007**, *25*, 119-130.

[14] Unpublished observations

[15] S. V. Ley, D. K. Baeschlin, D. J. Dixon, A. C. Foster, S. J. Ince, H. W. M. Priepke, D. J. Reynolds, *Chem. Rev*. **2001**, *101*, 53-80.

[16] I. C. S. Wan, M. D. Witte, A. J. Minnaard, *Org. Lett*. **2019**, *21*, 7669-7693.

[17] S. Youssif, *Arkivoc*, **2001**, *(i)*, 242-268.

[18] R. Andreozzi, A. Insola, V. Caprio, M. G. D'Amore, *Water Res*. **1991**, *25*, 655-659.

[19] Ozone can be generated thermally from air in the presence of metal oxides: A. N. Romanov, Y. N. Fattakhova, Y. N. Rufov, *Khimicheskaya Fizka*, **1998**, *17*, 85-90.
[20] The thermal production of hydrogen peroxide from oxygen and certain organic compounds has been reported: P. A. Clapp, N. Du, D. F. Evans, *J. Chem. Soc., Faraday Trans.* **1990**, *86*, 2587-2592.
[21] M. Shiramizu, F. D. Toste, *Angew. Chem. Int. Ed*. **2012**, *51*, 8082-8086.
[22] W. C. Still, M. Kahn, A. Mitra, *J. Org. Chem.* **1978**, *43*, 2923-2925.
[23] A. B. Pangborn, M. A. Giardello, R. H. Grubbs, R. K. Rosen, F. J. Timmers, *Organometallics* **1996**, *15*, 1518-1520.
[24] D. Aragao, J. Aishima, H. Cherukuvada, R. Clarken, M. Clift, N. P. Cowieson, D. J. Ericsson, C. L. Gee, S. Macedo, N. Mudie, S. Panjikar, J. R. Price, A. Riboldi-Tunnicliffe, R. Rostan, R. Williamson, T. T. Caradoc-Davies *J. Synchrotron Rad*. **2018**, *25*, 885-891.
[25] CrysAlis PRO Version 1.171.37.35h (release 09-02-2015 CrysAlis171.NET) (compiled Feb 9 2015,16:26:32) Agilent Technologies: Oxfordshire, UK.
[26] G. M. Sheldrick, *Acta Cryst*. **2015**, *A71*, 3-8
[27] G. M. Sheldrick, *Acta Cryst*. **2015**, *C71*, 3-8.
[28] Y. Zhao, D. G. Truhlar, *Theoretical Chemistry Accounts* **2008,** *120*, 215-241.
[29] I. Alecu, J. Zheng, Y. Zhao, D. G. Truhlar, *J. Chem. Theory Computation* **2010,** *6*, 2872-2887.
[30] L. A. Curtiss, K. Raghavachari, P. C. Redfern, A. G. Baboul, J. A. Pople, *Chem. Phys. Lett.* **1999,** *314*, 101-107.
[31] Gaussian 16, Revision C.01, M. J. Frisch, G. W. Trucks, H. B. Schlegel, G. E. Scuseria, M. A. Robb, J. R. Cheeseman, G. Scalmani, V. Barone, G. A. Petersson, H. Nakatsuji, X. Li, M. Caricato, A. V. Marenich, J. Bloino, B. G. Janesko, R. Gomperts, B. Mennucci, H. P. Hratchian, J. V. Ortiz, A. F. Izmaylov, J. L. Sonnenberg, D. Williams-Young, F. Ding, F. Lipparini, F. Egidi, J. Goings, B. Peng, A. Petrone, T. Henderson, D. Ranasinghe, V. G. Zakrzewski, J. Gao, N. Rega, G. Zheng, W. Liang, M. Hada, M. Ehara, K. Toyota, R. Fukuda, J. Hasegawa, M. Ishida, T. Nakajima, Y. Honda, O. Kitao, H. Nakai, T. Vreven, K. Throssell, J. A. Montgomery, Jr., J. E. Peralta, F. Ogliaro, M. J. Bearpark, J. J. Heyd, E. N. Brothers, K. N. Kudin, V. N. Staroverov, T. A. Keith, R. Kobayashi, J. Normand, K. Raghavachari, A. P. Rendell, J. C. Burant, S. S. Iyengar, J. Tomasi, M. Cossi, J. M. Millam, M. Klene, C. Adamo, R. Cammi, J. W. Ochterski, R. L. Martin, K. Morokuma, O. Farkas, J. B. Foresman, and D. J. Fox, Gaussian, Inc., Wallingford CT, 2016.
[32] MOLPRO is a package of ab initio programs written by H.-J. Werner, P. J. Knowles, G. Knizia, F. R. Manby, M. Schütz, P. Celani, W. Györffy, D. Kats, T. Korona, R. Lindh, A. Mitrushenkov, G. Rauhut, K. R. Shamasundar, T. B. Adler, R. D. Amos, S. J. Bennie, A. Bernhardsson, A. Berning, D. L. Cooper, M. J. O. Deegan, A. J. Dobbyn, F. Eckert, E. Goll, C. Hampel, A. Hesselmann, G. Hetzer, T. Hrenar, G. Jansen, C. Köppl, S. J. R. Lee, Y. Liu, A. W. Lloyd, Q. Ma, R. A. Mata, A. J. May, S. J. McNicholas, W. Meyer, T. F. {Miller III}, M. E. Mura, A. Nicklaß, D. P. O'Neill, P. Palmieri, D. Peng, K. Pflüger, R. Pitzer, M. Reiher, T. Shiozaki, H. Stoll, A. J. Stone, R. Tarroni, T. Thorsteinsson, M. Wang, M. Welborn